ARTICLES

Solid-State NMR Study of an Open-Framework Aluminophosphate-Oxalate Hybrid

Gregor Mali,*,† Nevenka Rajić,†,‡ Nataša Zabukovec Logar,† and Venčeslav Kaučič†,§

National Institute of Chemistry, Ljubljana, Slovenia, Faculty of Technology and Metallurgy, University of Belgrade, Yugoslavia, and University of Ljubljana, Slovenia

Received: July 9, 2002; In Final Form: November 27, 2002

Short-range order within a novel aluminophosphate-oxalate hybrid material with the unit cell formula $CH_2(NH_3)CH(NH_3)CH_3Al_4P_6O_{20}(OH)_4(C_2O_4)H_2O$ was studied by multinuclear solid-state NMR measurements. The ^{13}C, ^{27}Al, and ^{31}P MAS NMR spectra showed several resonance lines that could not be predicted by the single-crystal X-ray diffraction analysis. The underlying variety of carbon, aluminum, and phosphorus local environments was due to the nonuniform arrangement of the protonated 1,2-diaminopropane species and water molecules residing within the pores of the open-framework material. $^1H\rightarrow{}^{13}C$ CPMAS NMR spectrum evidenced that the diaminopropane species either occupied two different positions or were present as two different isomers, which also gave rise to two slightly different deformations of one ($P(3)O_4$) of the three crystallographically distinct PO_4 tetrahedra. One-dimensional ^1H and ^{31}P MAS and 2D $^1H\rightarrow{}^{31}P$ CPMAS spectra revealed that the water molecule, occupying a well-defined position within the pore with about 42% abundance, attracted H(2) from the hydroxyl group attached to the P(3) atom and involved the hydrogen atom into a strong hydrogen bond. The displacement of H(2) due to the interaction with the water molecule was determined by measuring H(2)−P(3) distances using $^1H\rightarrow{}^{31}P$ variable-contact-time CPMAS NMR experiments. As evidenced by ^{27}Al MAS and 3QMAS NMR spectra, the deformation of the $P(3)O_4$ tetrahedra by water and diaminopropane species further affected also local environments of the two proximal crystallographically inequivalent aluminum sites Al(1) and Al(2).

1. Introduction

The domain of porous solids has been a subject of extensive studies over the last few decades. The burst of the domain started with zeolites[1] and alumino-[2] and gallophosphates.[3] In these materials the framework is inorganic and the organic components act as templates around which the porous structure is generated. The discovery of hybrid porous solids[4] in which the framework is built of both organic and inorganic moieties, strongly connected by covalent bonds, gave a new impact to the domain. The introduction of organic components, namely, raises the possibility of tuning the dimensions of the pores through the selection of organic chains of the proper length and shape.

Recently we have prepared a new inorganic−organic hybrid material[5] whose structure can be described with pillared inorganic layers. It has the unit cell formula $CH_2(NH_3)CH(NH_3)CH_3Al_4P_6O_{20}(OH)_4(C_2O_4)H_2O$ and crystallizes in the triclinic symmetry. The framework consists of aluminophosphate layers, with characteristic eight-member rings, linked together with oxalate units. The linkages between the aluminophosphate layers and oxalates furthermore give rise to uniform elliptical 12-member channels along the *b*-axis. The negatively charged framework is neutralized by the doubly protonated 1,2-diaminopropane species, which reside together with water molecules within the pores. The amine and water are also involved in a strong hydrogen bond network with the framework oxygen atoms.

Single-crystal X-ray diffraction analysis of the aluminophosphate-oxalate hybrid enabled the determination of the crystal structure and the location of the diaminopropane and water species within the pores. However, since the X-ray diffraction (XRD) relies on a long-range order, the determined atomic positions reflect only the averaged structural parameters. This was a stimulus for performing a detailed solid-state nuclear magnetic resonance (NMR) investigation in order to obtain a complementary insight into a short-range order. In particular, we investigate the interaction of the diaminopropane and water species with the aluminophosphate-oxalate framework on a local scale. The present work also demonstrates that using modern solid-state NMR techniques one can locate protons in powdered porous materials and thus yield information, which was not attainable by the X-ray powder diffraction analysis.

2. Experimental Section

The aluminophosphate-oxalate hybrid was prepared by hydrothermal crystallization from an aluminophosphate reaction system containing oxalic acid and 1,2-diaminopropane. The crystallization was carried out in a Teflon-lined stainless steel autoclave at 130 °C under autogenous pressure for 4 days. The details of the synthesis are described in ref 5. Solid-state NMR

* Corresponding author. E-mail: gregor.mali@ki.si.
† National Institute of Chemistry.
‡ Faculty of Technology and Metallurgy.
§ University of Ljubljana.

10.1021/jp026469t CCC: $25.00
Published on Web 01/16/2003

TABLE 1: Details about MAS and CPMAS NMR Measurements

nuclei	ν_{RF1} [kHz]	ν_{RF2} [kHz]	pulse length/ contact time [μs]	delay [s]	number of scans
^{1}H	62.5		4	10	4
^{27}Al	65		1	5	100
^{31}P	30		5	150	200
^{1}H−^{13}C	56	46	8000	5	16000
^{1}H−^{31}P	30	20/15.6[a]	50−5000	5	16
^{27}Al−^{31}P	1	13	3000	1	12000

[a] Variable-contact-time ^{1}H→^{31}P CPMAS measurements were carried out at two different MAS frequencies (10 and 14.4 kHz) and correspondingly two different radio-frequency-field adjustments.

TABLE 2: Space Group and Unit Cell Parameters of the Aluminophosphate-Oxalate Hybrid

space group	$P\bar{1}$	
$a = 0.86110(10)$ nm	$b = 0.90960(10)$ nm	$c = 1.13710(10)$ nm
$\alpha = 104.8110(10)°$	$\beta = 111.3680(10)°$	$\gamma = 94.2480(10)°$
$V = 0.78791(14)$ nm^3		
$Z = 2$		

experiments were performed on a narrow-bore Varian Unity Inova spectrometer operating at 150.87, 156.35, 242.89 and 600.03 MHz for the ^{13}C, ^{27}Al, ^{31}P, and ^{1}H nuclei, respectively. For all MAS, CPMAS, and MQMAS measurements on the aluminophosphate-oxalate a Doty triple-tuned CPMAS probehead was used. The sample was spun with a spinning speed between 10 and 15 kHz. Some details on multinuclear MAS and CPMAS measurements are presented in Table 1.

3. Results and Discussion

The structure of the aluminophosphate-oxalate hybrid is schematically shown in Figure 1 and some crystal structure data are listed in Table 2. In each inorganic layer of the aluminophosphate-oxalate there are three crystallographically distinct PO_4 tetrahedra, an AlO_4 tetrahedron, and an AlO_6 octahedron. The aluminophosphate layer with characteristic eight-member rings can be viewed also as an ensemble of inter-connected double chains, which are composed of phosphorus atoms occupying tetrahedral sites P(1) and P(2), and aluminum atoms residing in tetrahedral sites Al(1) and octahedral sites Al(2). The double chains are interconnected through Al(1)−O−P(3)−O−Al(2) bridges. Each octahedrally coordinated aluminum atom is additionally bonded to two oxygens of an oxalate group through which neighboring inorganic layers are linked into a three-dimensional inorganic−organic hybrid structure. An asymmetric unit of the aluminophosphate-oxalate contains one doubly protonated diaminopropane molecule and one water molecule (with the probability of 42% ± 2%), both residing between the aluminophosphate layers close to Al(1)−O−P(3)−O−Al(2) linkages.

We begin the investigation of a short-range order within the aluminophosphate-oxalate with MAS NMR spectrum of aluminum nuclei (Figure 2). The spectrum shows two clearly resolved contributions of equal intensities. The narrower contribution at about 42 ppm and the broader contribution between −3 and −15 ppm lie within typical regions of signals of tetrahedrally and octahedrally coordinated aluminum nuclei, respectively, and thus completely agree with the structure determined by the single-crystal XRD.

The spectrum of phosphorus nuclei is somewhat surprising (Figure 3a). Although all three crystallographically distinct phosphorus sites are tetrahedrally coordinated, their local environments mutually differ and accordingly, the corresponding NMR signals are expected to be well resolved. Thus, two of

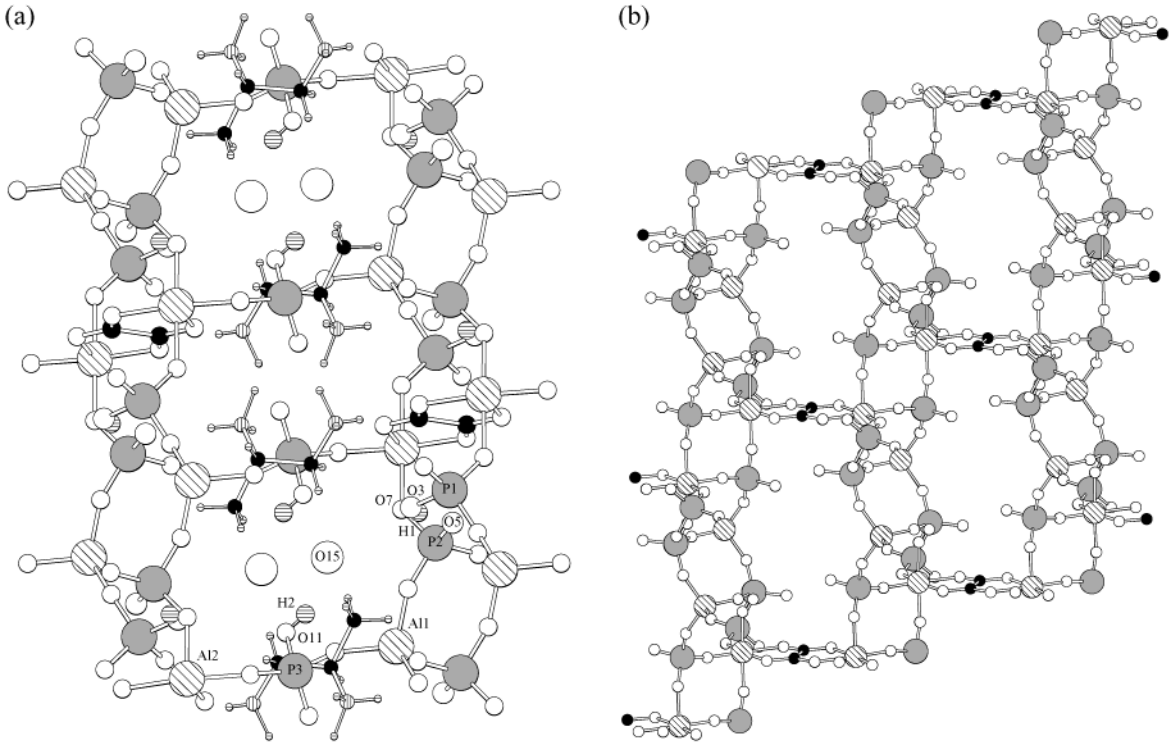

Figure 1. The structure of the aluminophosphate-oxalate hybrid. (a) View along *a*-axis shows that double chains built of $Al(1)O_4$, $Al(2)O_6$, $P(1)O_4$, and $P(2)O_4$ polyhedra are interconnected through Al(1)−O−P(3)−O−Al(2) linkages. Close to the linkages 1,2-diaminopropane and water (O(15)) species are located. Oxygen, phosphorus, and aluminum atoms are represented by white, gray, and dashed (slanted) circles, whereas carbon, nitrogen, and hydrogen atoms are shown as black, vertically dashed, and horizontally dashed circles, respectively. (b) View along *b*-axis schematically shows that the aluminophosphate layers are linked together with oxalate units. Diaminopropane and water species as well as hydrogen atoms were omitted from the figure for clarity.

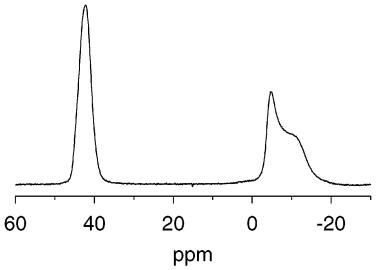

Figure 2. ^{27}Al MAS NMR spectrum of the aluminophosphate-oxalate hybrid.

the three crystallographically inequivalent PO_4 tetrahedra consist of three bridging and one terminal oxygen atoms. For the P(1)O_4 tetrahedron the terminal oxygen belongs to a hydroxyl group, whereas for the P(2)O_4 tetrahedron the terminal oxygen forms a double bond to P(2). The third tetrahedron P(3)O_4 consists of two bridging oxygen atoms, a terminal oxygen from a hydroxyl group, and a double-bonded terminal oxygen. Contrary to three crystallographically inequivalent phosphorus sites it is five contributions that can be resolved in the spectrum of phosphorus nuclei. Equal intensities of the resonance line at −20.6 ppm, the resonance line at −18.4 ppm, and the sum of the remaining three resonance lines suggest that the last three contributions with resonances at −12.1, −8.9, and −2.7 ppm belong to phosphorus nuclei occupying crystallographically equivalent but magnetically inequivalent sites.

The assignment of NMR signals to the three crystallographically distinct sites is most convincingly accomplished by the ^{27}Al→^{31}P double-resonance NMR measurements. By employing a very weak radio frequency field on the aluminum channel (see Table 1) and centering the carrier frequency of that channel to either Al(1) or Al(2) resonance, it is possible to selectively transfer polarization to phosphorus nuclei from either tetrahedrally or octahedrally coordinated aluminum nuclei.[6] The most prominent difference between the ^{27}Al (1)→^{31}P and ^{27}Al (2)→^{31}P CPMAS spectra (Figure 3b) is that in the first spectrum the resonance line at −18.4 ppm is twice as intense as the resonance line at −20.6 ppm, whereas in the second spectrum the ratio of the corresponding intensities is inverted. According to the single-crystal structure determination, the P(1) atom is through oxygen connected to one Al(1) and two Al(2) atoms, while a P(2) atom is connected to two Al(1) and one Al(2) atoms. It thus follows that phosphorus resonances at −20.6 and −18.4 ppm have to be assigned to the sites P(1) and P(2), respectively. The intensity of the resonance line at −2.7 ppm is in both double-resonance spectra equal, which agrees with the fact that P(3) is surrounded by a single Al(1) and a single Al(2) atom. In accord with the previous discussion the remaining two weak resonances shall be assigned to the nuclei that occupy sites P(3) with slightly different local environments. To make a clear distinction among the three magnetically inequivalent P(3) environments, in the ensuing text the nuclei with resonances at −2.7, −8.9, and −12.1 ppm are denoted as P(3)a, P(3)b, and P(3)c, respectively.

The diversity of local environments corresponding to the P(3) site explains why the crystallographically determined temperature factors for the P(3) atom position, and especially for positions of its terminal oxygen atoms are about twice or three times as large as the factors for the rest of phosphorus or oxygen positions.[5] A qualitative explanation of the presence of different P(3) environments might be obtained by looking at Figure 1, where it can be noticed that among all the phosphorus and aluminum sites this site is the closest one to the water molecule in the position represented by O(15). Since the later is occupied

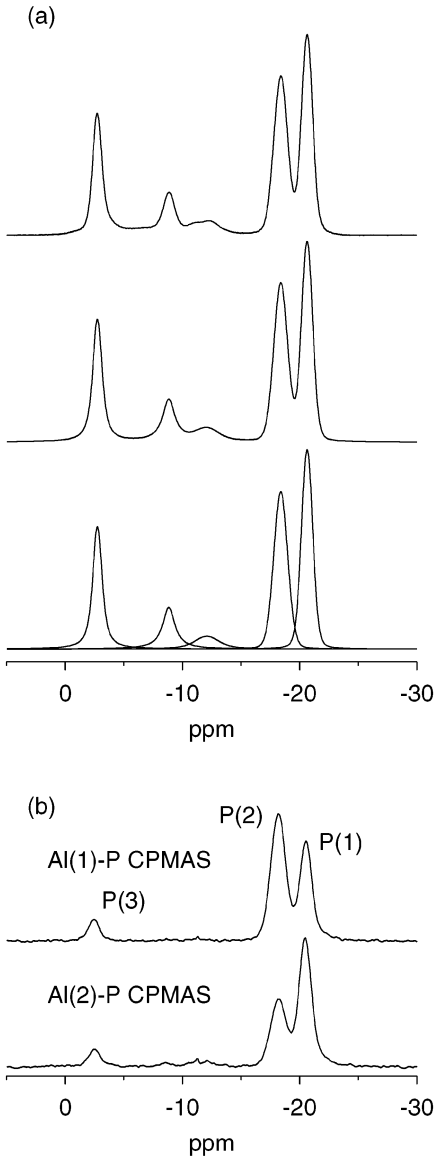

Figure 3. ^{31}P MAS NMR. (a) Measured phosphorus spectrum, the sum of decomposed lines, and individual lines in the decomposition of the phosphorus spectrum follow from top to bottom. (b) The top and the bottom ^{27}Al→^{31}P CPMAS spectra were obtained by a selective transfer of polarization from tetrahedrally and octahedrally coordinated aluminum nuclei, respectively.

with only about 42% probability, it is reasonable to expect that the presence or absence of the water molecule affects the P(3)O_4 tetrahedron differently. Such an explanation, however, still leaves the question of why there are three instead of only two signals belonging to P(3) nuclei.

The individual intensities of the P(3)a, P(3)b, and P(3)c NMR signals offer some additional insight into the P(3) environments and provide also some support to the above suggestion. Namely, the intensity of the P(3)a signal represents 57%±3% of the intensity of the entire P(3) signal. This is very close to the probability (58%) that the water molecule is absent from the vicinity of the P(3). The decomposition of relatively weak and slightly overlapped P(3)b and P(3)c signals resolves their contributions as 28%±3% and 15%±3% to the total P(3) signal, respectively. While these intensities are not very informative and reliable, the overlapping signals indicate that P(3)bO_4 and P(3)cO_4 tetrahedra are relatively similar to one another and that the perturbation inducing this small difference is weaker than

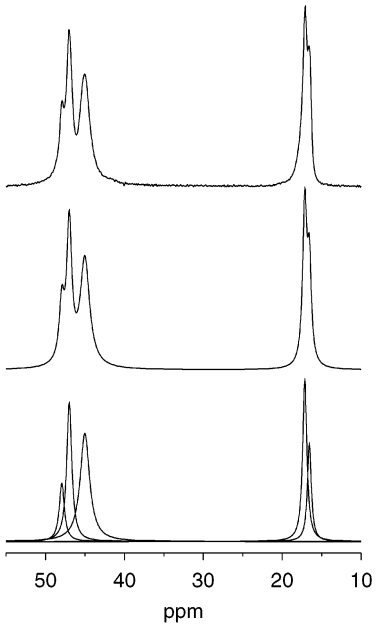

Figure 4. $^{1}H \rightarrow ^{13}C$ CPMAS NMR. Measured carbon spectrum, the sum of decomposed lines, and individual lines in the decomposition of the carbon spectrum follow from top to bottom. Only the part of the spectrum with resonances belonging to carbon from doubly protonated 1,2-diaminopropane molecules is shown.

the perturbation inducing the difference between the P(3)aO_4 tetrahedron on one side and P(3)bO_4 and P(3)cO_4 tetrahedra on the other.

A possible source of the weaker perturbation of the P(3) environment could be the diaminopropane species, which are also very close to the P(3) atoms. To examine this possibility we recorded the spectrum of the carbon nuclei in the aluminophosphate-oxalate hybrid. Beside a narrow resonance line at 168 ppm belonging to carbon nuclei from oxalate groups (not shown), three major contributions at about 47, 45, and 17 ppm (shown in Figure 4) can be assigned to the carbon nuclei in CH_2NH_3 groups, $CHNH_3$ groups, and CH_3 groups of the protonated 1,2-diaminopropane species. Although the structural data obtained by the single-crystal determination predict single crystallographic site for each of these carbons, the NMR signals of the "outer" carbons are both split into two resonance lines (47.9 and 47.0 ppm for the carbon in CH_2NH_3 groups, and 17.1 and 16.6 ppm for the carbon in CH_3 groups). This indicates that the protonated 1,2-diaminopropane species either occupy two different positions or, since the 1,2-diaminopropane is chirally active, it is present as isomers. The presence of different isomers could be justified if the commercial compound, used in the preparation of the sample, was a racemat. Two different positions or isomers of the diaminopropane species can induce two slightly different environments of the neighboring P(3) atoms. Indeed, the decomposition of both split carbon lines shows that the ratio of occupancies of the two positions or isomers is about 2:1 (68%±3%:32%±3% for CH_2NH_3 and 65%±9%:35%±9% for CH_3), which is reasonably close to the ratio of intensities of P(3)b and P(3)c NMR signals.

The above hypotheses about the influence of water and diaminopropane species on the local environment of the P(3) site rely mostly on the intensities of individual phosphorus and carbon resonance lines. Because the intensities obtained by the decomposition of strongly overlapped signals are sometimes not very reliable, we tried to obtain an additional information about the interaction between the framework and the species residing within the pores of the aluminophosphate-oxalate lattice by

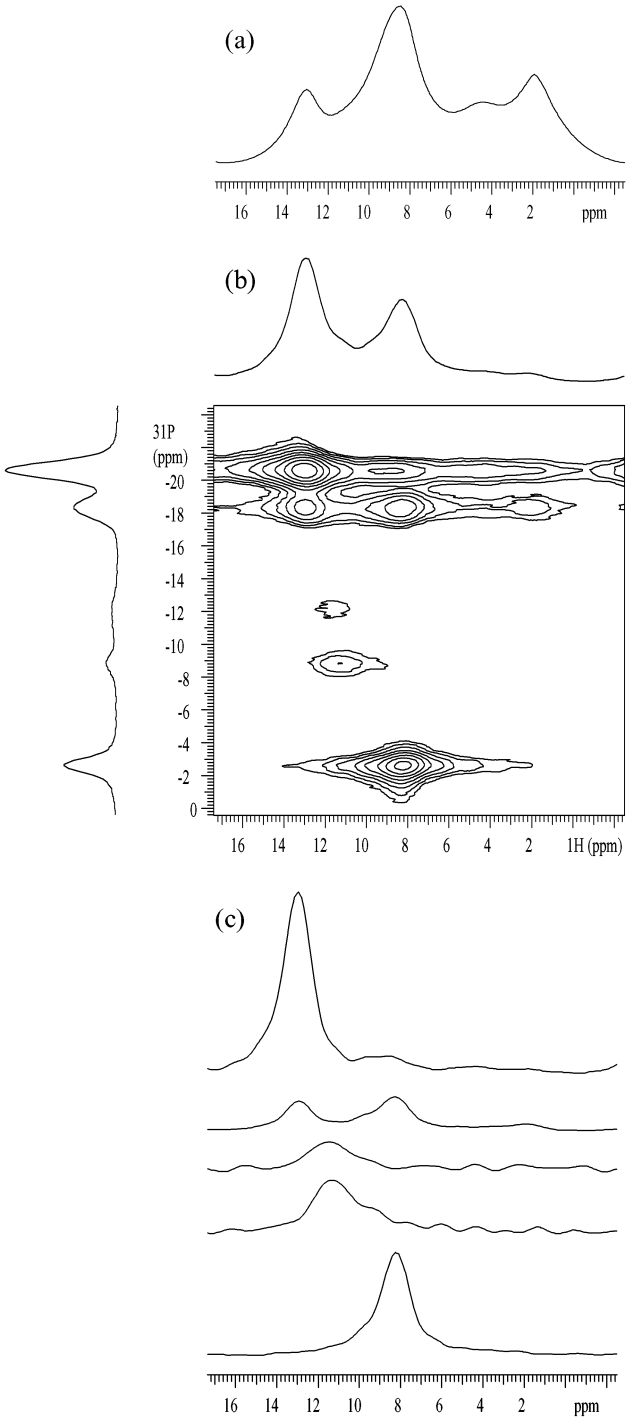

Figure 5. ^{1}H MAS and $^{1}H \rightarrow ^{31}P$ CPMAS NMR. (a) 1D proton spectrum, (b) 2D CPMAS spectrum elucidating the proximity among particular phosphorus and proton sites, and (c) slices along ^{1}H axis taken from the 2D spectrum at different frequencies in ^{31}P dimension. From top to bottom the slices were taken at −20.5, −18.3, −12.1, −8.9, and −2.7 ppm thus showing cross-sections through P(1), P(2), P(3)c, P(3)b, and P(3)a cross-peaks, respectively.

measuring 1D ^{1}H MAS and 2D $^{1}H \rightarrow ^{31}P$ CPMAS spectra (Figure 5). In the proton spectrum at least four different contributions can be resolved. The peaks at 1.9 and 4.4 ppm can be assigned to protons in aliphatic groups and water molecules, respectively, whereas the overlapping signals between 7 and 14 ppm might belong to the protons in amino and hydroxyl groups that are involved in hydrogen bond network. In the 2D CPMAS measurement a very short contact time of 200 μs was employed, so that only the polarization from the nearest protons was

TABLE 3: Distances between the Averaged Phosphorus Positions and nearest Protons[a]

$d_{P(1)-H}$ [nm]	$d_{P(2)-H}$ [nm]	$d_{P(3)-H}$ [nm]
H(1) 0.190(6)	H(8) 0.295(4)	H(2) 0.194(12)
H(4) 0.323(7)	H(1) 0.306(6)	H(6) 0.290(5)
H(11) 0.338(5)		H(3) 0.295(6)
		H(7) 0.304(5)
		H(5) 0.317(9)

[a] All protons that are less than 0.35 nm distant from a phosphorus position are listed. Protons H(1) and H(2) belong to terminal hydroxyl groups attached to P(1) and P(3), respectively; H(3−8) belong to amino groups and H(9−14) belong to aliphatic groups. Standard deviation on the last decimal number is given in parentheses.

efficiently transferred to the phosphorus nuclei. In agreement with the single-crystal structure determination (the distances between the three averaged phosphorus positions and nearest protons are listed in Table 3), there are two very strong cross-peaks in the 2D spectrum due to the P(1)−O(3)−H(1) and P(3)a−O(11)−H(2) bonds. A relatively large difference between the chemical shifts of H(1) protons (13.0 ppm) and H(2) protons (8.5 ppm) probably results from the fact that the H(1) is involved in a very strong hydrogen bond with O(5) which is doubly bonded to P(2). The O(3)−O(5) distance is only 0.2534 nm ± 0.0004 nm. In the absence of the water molecule the H(2) might be involved in a weaker hydrogen bond to O(7). The distance between the averaged O(11) position and O(7) is 0.2970 nm ± 0.0005 nm.

The crucial observation connected with the 2D $^{1}H\rightarrow{}^{31}P$ CPMAS measurement is the presence of relatively strong cross-peaks between P(3)b and P(3)c on one hand, and magnetically equivalent protons resonating at 11.4 ppm on the other. The observation implies three important conclusions. First, strong cross-peaks indicate that the two phosphorus sites are indeed sites with an attached terminal hydroxyl group, which confirms the assignment of these two phosphorus resonances to the perturbed P(3) sites. Second, the environment of the H(2) proton attached to P(3)a is different from the environments of the protons H(2) attached to either P(3)b or P(3)c. The shift of the H(2) resonance from 8.5 to 11.4 ppm shows that in the later case the H(2) protons are involved in a stronger hydrogen bond, confirming that the major perturbation displacing the P(3)b and P(3)c resonances from the P(3)a resonance is the appearance of the water molecule in position O(15). Although the exact positions of the H(2) and O(11) atoms most probably vary among the different P(3) environments, the averaged H(2)−O(15) and O(11)−O(15) distances of 0.17 ± 0.01 nm and 0.245 ± 0.001 nm, respectively, still indicate that in the cases of P(3)b and P(3)c a strong hydrogen bond O(11)−H(2)···O(15) is formed. Finally, the magnetic equivalence of the protons H(2) attached to P(3)b and P(3)c suggests that the small difference between these two phosphorus environments is not caused by water in O(15) position but by another species, most probably the diaminopropane.

A continuous development of the solid-state NMR spectroscopy lately led to the introduction of techniques that in some cases provide not only qualitative information about connectivities within inorganic solids but also the quantitative information about internuclear distances. In rotating polycrystalline samples heteronuclear distances are most often measured by the rotational echo double resonance (REDOR) method.[7] Recently, as an alternative, the CP technique was employed for determining the $^{27}Al-{}^{1}H$, $^{27}Al-{}^{31}P$, and $^{1}H-{}^{31}P$ distances in the as-synthesized and calcined $AlPO_4-31$,[6] and in cubane-shaped molecular aluminophosphates,[8] respectively. In the absence of spin diffusion the time-domain signals of both methods build up in an oscillatory manner, which reflects the geometry of the investigated spin system.[9] However, in polycrystalline samples CP should exhibit more pronounced long-term oscillations than REDOR.

Results of the variable-contact-time CP measurements in the aluminophosphate-oxalate hybrid rotating at 10 and 14.4 kHz are presented in Figure 6a,b, respectively. Faster sample rotation suppresses spin-diffusion among protons more efficiently and thus slightly simplifies the analysis of time-domain signals. Otherwise the results of both measurements are very similar. They clearly show that the cross-polarization from protons to the P(1) and P(3)a nuclei is a mixture of a coherent polarization transfer from strongly coupled protons H(1) and H(2), respectively, producing fast initial rise of the signals and their oscillatory behavior, and an incoherent polarization transfer from the remote protons, producing smooth time-domain evolution. In the absence of terminal hydroxyl group the P(2) nuclei are, of course, polarized only from remote protons so that the corresponding signal exhibits no oscillations. The time-domain signal of the P(3)b nuclei is weaker but rather similar to the P(3)a signal, also exhibiting a combination of coherent and incoherent polarization transfer. The signal of the P(3)c nuclei is still weaker and not shown here. Its analysis is not reliable due to poor signal-to-noise ratio.

The time-domain oscillations in P(1), P(3)a, and P(3)b CPMAS signals decay rather fast, which makes the determination of the $^{1}H-{}^{31}P$ internuclear distances from the Fourier transforms of time-domain signals difficult. Namely, the decay of oscillations inhomogeneously broadens and lowers the Pake-like doublet in the Fourier transformed signal, so that the determination of the splitting of the doublet may become inaccurate.[6,10] Therefore, we extracted the magnitudes of the $^{1}H-{}^{31}P$ couplings by fitting time-domain signals with the function[9]

$$\langle S_x\rangle(t) = [\exp(-t/T_{1\rho}) - \exp(-k_1 t)g_n(t)] + \frac{N-1}{N+1}[\exp(-t/T_{1\rho}) - \exp(-k_2 t)] \quad (1)$$

The expression above describes the time evolution of the CP signal in a "real" isolated spin system which consists of a strongly coupled $^{1}H-{}^{31}P$ spin pair and $N-1$ weakly coupled (remote) ^{1}H spins. $T_{1\rho}$ is the dominant relaxation time and k_1 and k_2 are the first-order rate constants that describe the decay of transient oscillations and the spin diffusion with remote ^{1}H spins. In the case of an ideal isolated spin pair ($N = 1$), the second term in the above expression describing spin diffusion vanishes. The function $g_n(t)$ describes the oscillatory behavior of the ^{31}P-spin polarization in a powder. The exact powder average at the first sideband matching condition ($n = \pm 1$) can be expressed in terms of Bessel functions of the first kind as[9]

$$g_{\pm 1}(t) = J_0\left(\frac{\pi\nu_D t}{\sqrt{2}}\right) + 2\sum_{k=1}^{\infty}\left[\frac{1}{1-4(2k)^2}J_{2k}\left(\frac{\pi\nu_D t}{\sqrt{2}}\right)\right] \quad (2)$$

The above expressions allow efficient nonlinear least-squares fitting of the experimental data.

The internuclear distances obtained from the fitting are 0.207 ± 0.002 nm for H(1)−P(1), 0.208 ± 0.002 nm for H(2)−P(3)a, and 0.215 ± 0.004 nm for H(2)−P(3)b. All distances are slightly larger than the distances determined by XRD. It is important to note that the H(2)−P(3)b distance is larger than the H(2)−P(3)a distance, which again suggests that the water

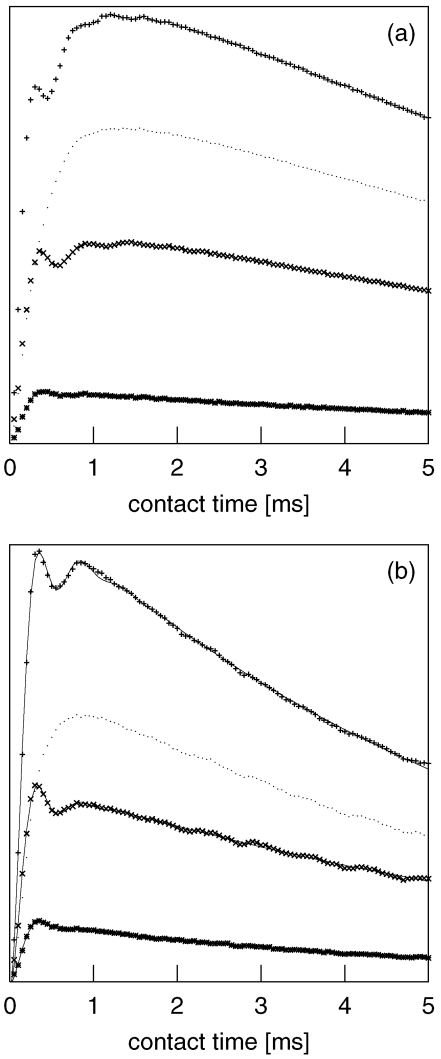

Figure 6. $^{1}H \rightarrow ^{31}P$ variable-contact-time CPMAS signals recorded in the aluminophosphate-oxalate sample rotating with (a) 10 kHz and (b) 14.4 kHz. Measured P(1), P(3)a, and P(3)b CPMAS signals are presented with +, ×, and ∗, respectively, dots show measured P(2) CPMAS signals and solid lines in (b) show fitted functions.

molecule in the vicinity of P(3)b attracts H(2) and involves it into the hydrogen bond.

The study will be concluded by returning to the spectrum of aluminum nuclei. So far we have seen that the partial occupancy of the water position O(15) and/or two possible positions (or isomers) of doubly protonated 1,2-diaminopropane are reflected in the ^{13}C, ^{1}H, ^{31}P, and $^{1}H \rightarrow ^{31}P$ (CP)MAS NMR spectra. A closer look shows that the spectrum of aluminum nuclei is also affected by the molecules residing within the pores of the aluminophosphate-oxalate hybrid. For example, the octahedral signal in Figure 2 suggests that it is composed of at least two contributions, because its shape does not correspond to any regular second-order quadrupolar line shape. A more firm evidence for the presence of different Al(1) and Al(2) environments can be seen in Figure 7. The 3QMAS[11] spectrum surprisingly does not improve the resolution of the octahedral signal but clearly shows the presence of two tetrahedral signals of unequal intensity. On the other hand, a set of the 1D ^{27}Al MAS spectra recorded with an initial pulse of varying length does show that the broad signal between −3 and −15 ppm is composed of several lines. In fact, the octahedral contributions in all five spectra in Figure 7b can be described by three Gaussian lines of fixed position and width but of variable

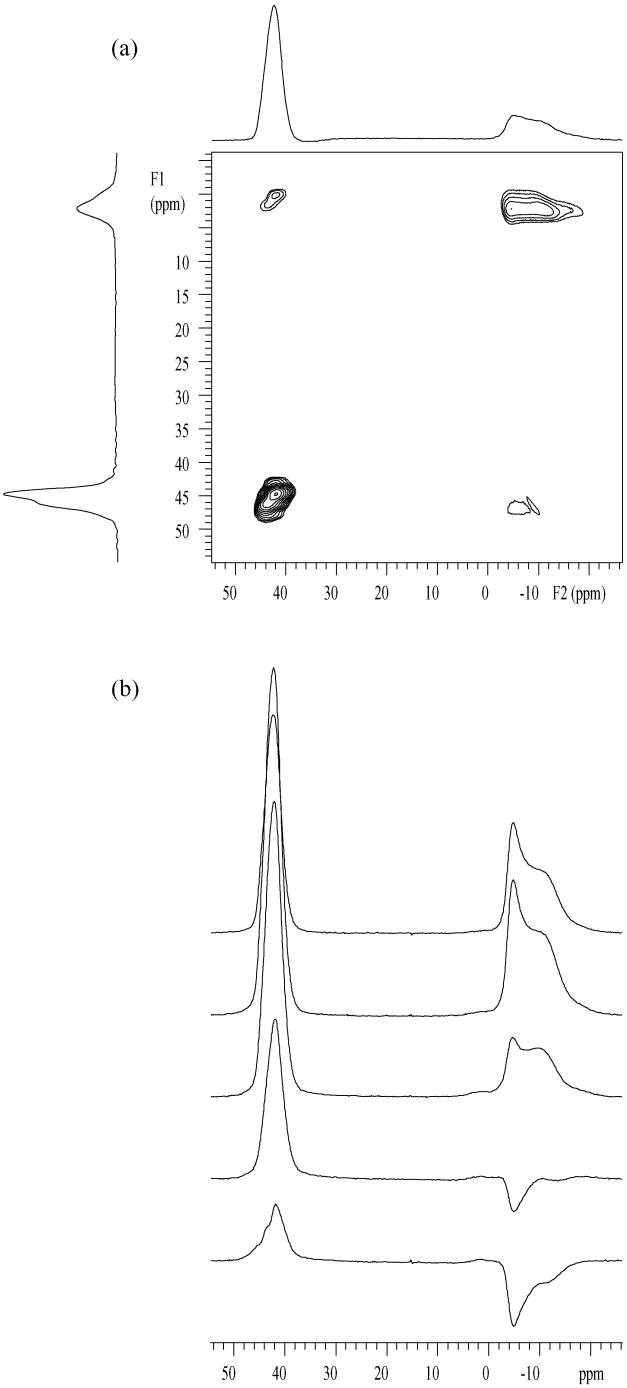

Figure 7. ^{27}Al MAS and 3QMAS NMR. (a) 2D sheared 3QMAS spectrum with the isotropic projection along F1 dimension. (b) 1D MAS spectra recorded with an initial pulse varying between 1 μs (top) and 5 μs (bottom).

intensities. The presence of several slightly different Al(1) and Al(2) environments is, of course, understandable because both sites are linked to the $P(3)O_4$ tetrahedron. If the later is perturbed by water and diaminopropane species, the $Al(1)O_4$ tetrahedron and $Al(2)O_6$ octahedron are indirectly affected as well.

4. Conclusions

NMR spectra of the aluminophosphate-oxalate hybrid show several resonance lines that could not be predicted by the single-crystal X-ray diffraction analysis. The underlying variety of carbon, aluminum, and phosphorus local environments is due to the nonuniform arrangement of the protonated diaminopro-

pane species and water molecules residing within the pores of the hybrid material. The diaminopropane species either occupy two different positions or are present as two different isomers and induce two slightly different deformations of the proximal $P(3)O_4$ tetrahedra. The water molecule, occupying a well-defined position within the pore with about 42% abundance, attracts H(2) from the hydroxyl group attached to the P(3) atom and incorporates the hydrogen atom into a strong hydrogen bond. The displacement of the H(2) due to the interaction with the water molecule was determined by the H(2)−P(3) NMR distance measurements. The deformation of the $P(3)O_4$ tetrahedra by water and diaminopropane species affects also $Al(1)O_4$ and $Al(2)O_6$ polyhedra.

Acknowledgment. The authors acknowledge the financial support of the Slovenian Ministry of Education, Science and Sport through research projects Z1-3277 and P0-0516-0104.

References and Notes

(1) Ozin, G. A.; Kuperman, A.; Stein, A. *Angew. Chem.* **1989**, *101*, 373.
(2) Wilson, S. T.; Lok, B. M.; Messina, C. A.; Cannan, T. R.; Flanigen, E. M. *J. Am. Chem. Soc.* **1982**, *104*, 1146.
(3) Estermann, M.; McCusker, L. B.; Baerlocher, C.; Merrouche, A.; Kessler, H. *Nature* **1991**, *352*, 320.
(4) Lightfoot, P.; Lethbridge, Z. A. D.; Morris, R. E.; Wragg, D. S.; Wright, P. A. *J. Solid State Chem.* **1999**, *143*, 74.
(5) Rajić, N.; Zabukovec Logar, N.; Mali, G.; Kaučič, V. *Chem. Mater*. Submitted for publication.
(6) Mali, G.; Kaučič, V. *J. Chem. Phys.* **2002**, *117*, 3327.
(7) Gullion, T.; Schaefer, J. *J. Magn. Reson.* **1989**, *81*, 196.
(8) Azaıs, T.; Bonhomme, C.; Bonhomme-Coury, L.; Vaissermann, J.; Millot, Y.; Man, P. P.; Bertani, P.; Hirschinger, J.; Livage, J. *J. Chem. Soc., Dalton Trans.* **2002**, 609.
(9) Fyfe, C. A.; Lewis, A. R.; Chezeau, J. M. *Can. J. Chem.* **1999**, *77*, 1984.
(10) Bertani, P.; Raya, J.; Reinheimer, P.; Gougeon, R.; Delmotte, L.; Hirschinger, J. *Solid State Nucl. Magn. Reson.* **1999**, *13*, 219.
(11) Frydman, L.; Harwood, J. S. *J. Am. Chem. Soc.* **1995**, *117*, 5367.